PHYSICAL REVIEW B **91**, 121112(R) (2015)

Real-time cumulant approach for charge-transfer satellites in x-ray photoemission spectra

J. J. Kas,[1] F. D. Vila,[1] J. J. Rehr,[1] and S. A. Chambers[2]
[1]*Department of Physics, University of Washington, Seattle, Washington 98195-1560, USA*
[2]*Physical Sciences Division, Pacific Northwest National Laboratory, Richland, Washington 99352, USA*
(Received 30 September 2014; revised manuscript received 23 February 2015; published 25 March 2015)

X-ray photoemission spectra generally exhibit satellite features beyond the main peak due to many-body excitations. However, the satellites associated with charge-transfer excitations in correlated materials have proved difficult to calculate from first principles and their interpretation has been controversial. Here we show that these satellites can be attributed to local density fluctuations in response to a suddenly created core hole. Our approach is based on a cumulant representation of the core-hole Green's function with a real-time, time-dependent density functional theory calculation of the cumulant. This approach includes effects that cannot be accounted for by cluster methods and yields a direct real-space, real-time interpretation. Illustrative results for TiO_2 and NiO are in good agreement with XPS experiment.

DOI: 10.1103/PhysRevB.91.121112 PACS number(s): 79.60.−i, 71.10.−w, 71.27.+a

Core-level x-ray photoemission spectroscopy (XPS) provides a direct probe of many-body excitations that characterize correlation effects in materials. These excitations are reflected in satellite features in the XPS photocurrent $J_{\boldsymbol{k}}(\omega)$ (see Fig. 1). Consequently, theories of XPS beyond the independent-particle approximation have been of considerable interest [1–11]. While there has been substantial progress in *ab initio* descriptions of plasmon satellites [12–14], the nature and interpretation of "charge-transfer" (CT) satellites has been controversial, e.g., in the early transition metal complexes, and first principles calculations have remained challenging. These localized excitations have been attributed to the response of a system to the sudden creation of a deep core hole. Schematically, the initial charge transfer from ligand to metal creates a "well screened" core hole that characterizes the main XPS peak, while the satellites at lower energies (Fig. 1) reflect charge-transfer back to the ligands and a more weakly screened core hole. Several frequency-space approaches have been introduced to treat this behavior. They include the single impurity Anderson model, charge-transfer multiplet theory, and semiempirical tight-binding models [15,16]. First principles methods, e.g., configuration interaction (CI), have also been used [17–20], but are computationally intensive and limited to small clusters of atoms. These latter methods cannot be used to determine details such as spatial extent of these excitations or their time evolution. On the other hand, the cumulant expansion has been found to explain the multiple-plasmon satellites in the XPS of weakly correlated systems [12–14,21]. These effects cannot be captured by local cluster methods or by the *GW* approximation of Hedin [22]. Moreover, the cumulant for the core-hole Green's function is directly related to local density response. It is therefore of interest to investigate whether the cumulant approach can be extended to treat the XPS of more correlated systems. We show here that this is indeed the case. Remarkably, this approach provides an efficient alternative for first principles calculations of CT satellites, as well as a physical understanding that gives a more definitive interpretation.

The cumulant method is based on an exponential representation of the core-hole Green's function $g_c(t)$ [23,24], and the

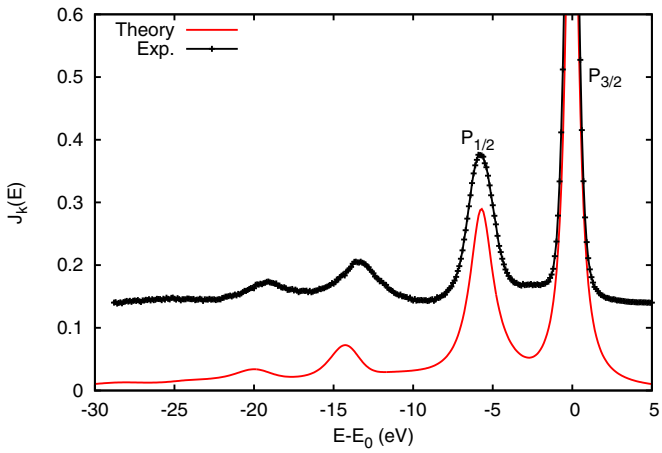

FIG. 1. (Color online) Comparison between the of the calculated Ti $2p_{3/2}$ and $2p_{1/2}$ XPS of rutile TiO_2 of this work (red) and experiment (black). Each of the spin-orbit split XPS peaks at 0 and −6 eV exhibits a strong charge-transfer satellite at an excitation energy $\omega_{\rm CT} \approx 14$ eV below. The plots are shifted vertically for clarity.

XPS photocurrent $J_{\boldsymbol{k}}(\omega)$ is roughly proportional to the spectral function $A_c(\omega)$, i.e.,

$$g_c(t) = g_c^0(t)e^{C(t)}, \quad g_c^0 = -\theta(-t)e^{-i\epsilon_c t}, \tag{1}$$

$$A_c(\omega) = -\frac{1}{\pi}\mathrm{Im}\int dt\, e^{i\omega t} g_c(t). \tag{2}$$

Here $C(t)$ is the cumulant, and $\theta(t)$ the unit step function; throughout this Rapid Communication we use atomic units $e = \hbar = m = 1$. Following Langreth [11,24], $C(t)$ can be approximated to second order in the core-hole potential by

$$C(t) = \sum_{\boldsymbol{q},\boldsymbol{q}'} V_{\boldsymbol{q}}^* V_{\boldsymbol{q}'} \int d\omega\, \mathrm{Im}[\chi(\boldsymbol{q},\boldsymbol{q}',\omega)] \frac{e^{i\omega t} - i\omega t - 1}{\omega^2}. \tag{3}$$

Here $V_{\boldsymbol{q}}$ is the core-hole potential in momentum space, and $\chi(\boldsymbol{q},\boldsymbol{q}',\omega)$ is the dynamic structure factor which is directly related to the density-density correlation function $\chi(\boldsymbol{q},\boldsymbol{q}',\omega) = i\int dt e^{i\omega t}\langle\rho_{\boldsymbol{q}}(t)\rho_{\boldsymbol{q}'}(0)\rangle\theta(t)$. This approach has its roots in the

theory of Nozières and de Dominicis for edge singularities in core-level x-ray spectra, where the cumulant is derived from the linked-cluster theorem [23]. Formally, the cumulant in Eq. (3) describes the transfer of spectral weight from the quasiparticle peak to a series of satellites with a spectral function that preserves spectral weight. For a deep hole coupled to ideal plasmons or bosons, this approximation is exact [24]; however, in general, corrections to the leading order cumulant will affect the higher order satellites. The time dependence $[\exp(i\omega t) - i\omega t - 1]/\omega^2$ arises from the transient core-hole potential, which turns on at time $t = 0$ and off at time t. The localized nature of the core hole has led us to consider a real-space, real-time approach that is not limited to small clusters. Here we adopt a real-time, time-dependent density functional theory formalism (RT-TDDFT) inspired by that of Bertsch and Yabana [25] for optical response. Such methods are advantageous for density response, as they are often semiquantitative, yet require little computational effort beyond ground state DFT. RT-TDDFT has been successfully applied both to linear and nonlinear optical response [26–29] as well as core-level x-ray absorption spectra ignoring satellites [30]. However, its application to the cumulant method or to CT excitations remains to be carried out.

Details of our theory are summarized below. We consider the excitation of an electron from a deep core level $|c\rangle$ to an unoccupied photoelectron state $\boldsymbol{k}$ by a high-energy x ray. The XPS photocurrent is given formally by the golden rule [1],

$$J_{\boldsymbol{k}}(\omega) = \sum_s |\langle N-1,s;\boldsymbol{k}|D|N\rangle|^2 \delta(\omega - \omega_s), \tag{4}$$

where $|N\rangle$ is the N electron ground state, $|N-1,s;\boldsymbol{k}\rangle$ is an excited state with the photoelectron and the $N-1$ electron system in excited state s, and D is the dipole operator. In general, one must consider all excitations due to interactions between valence electrons and the core hole (intrinsic) or the photoelectron (extrinsic), as well as interference terms [1]. However, since the localized CT excitations are primarily intrinsic, the photocurrent can be expressed in terms of the spectral functions $A_j(\omega)$, which we assume are diagonal in the core states $|j\rangle$,

$$J_{\boldsymbol{k}}(\omega) = \sum_j |\Delta_{\boldsymbol{k}j}|^2 A_j(\omega). \tag{5}$$

For deep core electrons and high-energy photoelectrons ($k \gg k_F$), the dipole matrix elements are roughly constant, so the contribution to the photocurrent from core level c is proportional to the core-hole spectral function $A_c(\omega) \propto J_{\boldsymbol{k}}(\omega)$, as given by Eq. (2). Transforming Eq. (3) to real space, we obtain

$$C(t) = \int d\omega\, \beta(\omega) \frac{e^{i\omega t} - i\omega t - 1}{\omega^2}, \tag{6}$$

$$\beta(\omega) = \int d^3r d^3r'\, V(\boldsymbol{r}) \mathrm{Im}[\chi(\boldsymbol{r},\boldsymbol{r}',\omega)] V(\boldsymbol{r}'). \tag{7}$$

The kernel $\beta(\omega)$ is the excitation spectrum of *effective* or charge-neutral "quasiboson" excitations [1]. Physically, this function is expected to exhibit peaks at the dominant excitations in $\chi(\boldsymbol{r},\boldsymbol{r}',\omega)$, and can be calculated in terms of the change in density $\delta\rho(\boldsymbol{r},t)$ induced by a core-hole potential turned on at $t = 0$,

$$\begin{aligned} \delta\rho(\boldsymbol{r},t) &= \int dt' d^3r'\, \chi(\boldsymbol{r},\boldsymbol{r}';t-t') V(\boldsymbol{r}')\theta(t'), \\ \Delta_c(t) &= \int d^3r\, V(\boldsymbol{r}) \delta\rho(\boldsymbol{r},t), \\ \frac{\beta(\omega)}{\omega} &= \mathrm{Re}\left[\int dt\, e^{-i\omega t} \Delta_c(t)\right]. \end{aligned} \tag{8}$$

Here $\Delta_c(t)$ reflects the oscillatory density response in the vicinity of the absorbing atom. In contrast to an optical response, $\Delta_c(t)$ is dominated by a monopole (i.e., s-like) response and has a qualitatively different spectrum. $\Delta_c(t)$ is related to the self-energy of the core electron, and $C'(0) = \int d\omega\, \beta(\omega)/\omega$ is the quasiparticle energy shift. Another correction to the energy of the main peak is the chemical shift [31]; we have ignored this effect since it does not change the shape of the spectral function.

We have implemented this theory within our RT-TDDFT extension of the SIESTA code [27]. The time evolution is carried out using a Crank-Nicolson propagator and an efficient basis of localized atomic orbitals [32,33]. For core levels where exchange with valence electrons can be neglected, the structure of the core hole is not crucial, so we have simply modeled $V(\boldsymbol{r})$ as a Yukawa potential flattened inside a small radius to avoid the singularity at $r = 0$. The response is then calculated by relaxing the system to its ground state, turning on $V(\boldsymbol{r})$ at $t = 0$, and then propagating the system to obtain $\delta\rho(\boldsymbol{r},t)$. In order to maintain linearity between the cumulant and $\delta\rho(\boldsymbol{r},t)$, we also rescale the potential and $\beta(\omega)$ accordingly. Finally, the Green's function and spectral function are formed according to Eqs. (2) and (3).

Figure 1 shows our calculated core-hole spectral function (red) for rutile TiO_2 compared to the measured XPS (black crosses). The spin orbit splitting is fixed at the experimental value, and a broadening parameter is introduced for each initial state to account for the intrinsic core-hole lifetime and experimental broadening. The two largest peaks at $\approx$0 and -6 eV correspond to the excitation of the $p_{1/2}$ and $p_{3/2}$ states (i.e., L_2 and L_3 edges), which are assumed to be independent. Each of these peaks has an associated CT satellite about 14 eV below, i.e., ≈ -14 and -20 eV, respectively. These dominant satellites are well reproduced by the calculations, albeit with slightly larger excitation energies. Since the higher order satellites are evidently weak, the leading order cumulant is adequate for this system.

Figure 2 illustrates the dynamic response. The top and middle panels show $\Delta_c(t)$ for a Ti core hole in rutile TiO_2 in real time (top) and in frequency space (middle). Although, in principle, one could calculate $C(t)$ directly from Eq. (3) using TDDFT or Bethe-Salpeter equation (BSE) calculations, the localized nature of the core hole makes our real-space implementation both advantageous and efficient. Interestingly, the dominant response for TiO_2 is characterized by a well defined CT excitation at $\omega_{CT} \approx 14$ eV (see the middle panel of Fig. 2). This behavior differs significantly from that for a core hole on the O atoms (dashed curve in the middle panel of Fig. 2), indicating that the dominant response is localized on the Ti atoms. The broad background is similar for both

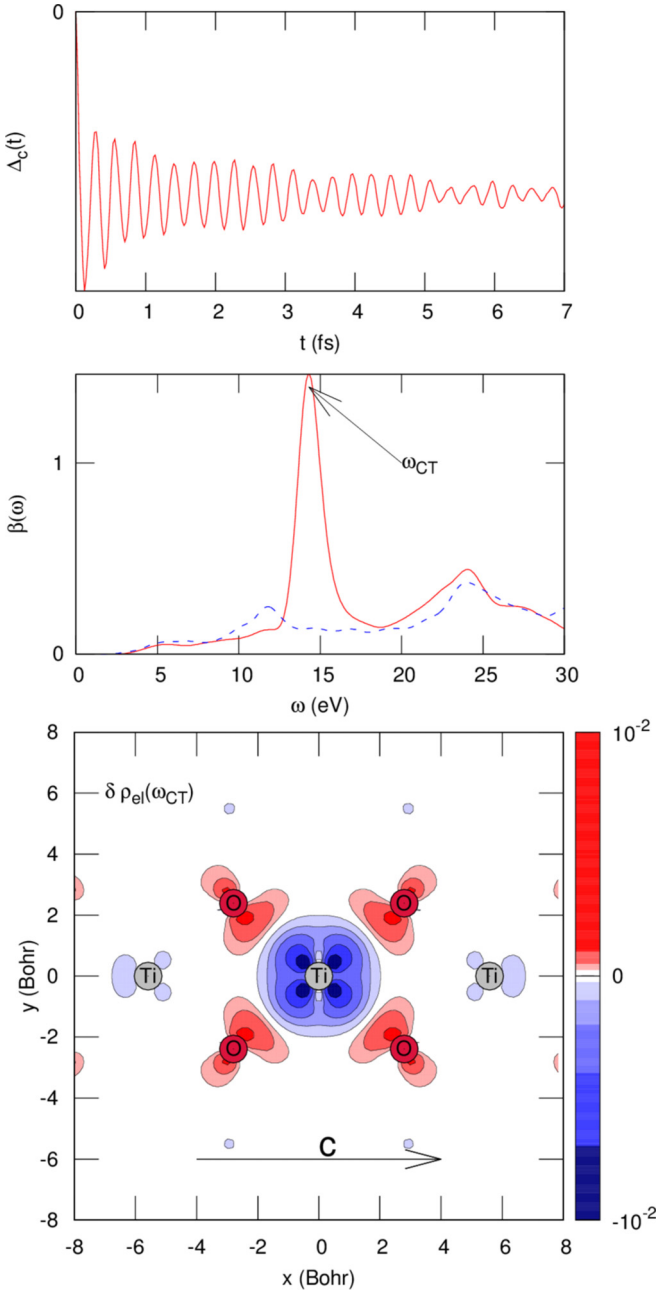

FIG. 2. (Color online) Top: Real-time Ti core-hole response function $\Delta_c(t)$ for TiO_2 vs t. Note the transient response in the first fraction of a femtosecond. Middle: Core excitation function $\beta(\omega)$ for a core hole on Ti (red) or O (blue dashed). Bottom: Excited state electron density $\delta\rho(\boldsymbol{r},\omega_{CT})$ in the Ti-O plane (see text) at the CT energy $\omega_{CT} \approx 14$ eV (see the arrow in the middle plot). The in-plane structure with the c axis along x is superimposed in the density plot.

Ti and O, and roughly comparable to the loss function for TiO_2 [34], consistent with delocalized plasmonlike excitations. Note also the pronounced transient response in the first few fs and the sharp decrease at the onset within a fraction of a fs. These features correspond to fast screening of the core hole by the valence electrons, followed by an oscillatory CT between metal and ligand atoms. The damping within the first few fs is due to the diffusion of the excitation into the surroundings. This effect requires the presence of an extended system and cannot be captured by local cluster models. The interpretation of the 14 eV satellite in TiO_2 is of considerable interest and has been controversial in the literature. Besides the CT interpretation [35], the 14 eV peak has been attributed to plasmonlike excitations, as observed in the loss function [34], or alternatively to intra-atomic excitons on the ligand [36] that characterize the polarization of ligand orbitals by the core-hole potential. However, the CT peaks in correlated materials such as CeO_2 have also been seen in the loss function [37,38]. These various interpretations reflect the fact that the concepts of plasmons and CT excitations are not mutually exclusive. This is not surprising, as both can be treated within a common density response formalism that couples to all density fluctuation excitations. Our results show that CT dominates for the main Ti satellite in TiO_2 but that polarization of the O ligands is clearly present (see Fig. 2). In order to demonstrate our interpretation spatially, we have plotted the Fourier transform $\delta\rho(\boldsymbol{r},\omega)$ at ω_{CT} (the bottom panel of Fig. 2), for points $\boldsymbol{r}$ in a plane through the Ti atom and the four nearest oxygen atoms. This plot clearly illustrates an oscillatory transfer of electrons between the Ti atom and the ligands during the CT process. In addition, the shape of the density fluctuations suggests CT from Ti $3d$ to hybridized O sp orbitals. This effect can be interpreted as a combined CT-polarization excitation due in part to intra-atomic electron-hole pairs on the ligand.

To demonstrate a wider applicability, similar calculations were carried out for NiO. NiO is more strongly correlated than TiO_2, as reflected in its larger net satellite weight $1 - Z = 0.81$ vs 0.37 for TiO_2, where $Z = \exp[-\int d\omega\, \beta(\omega)/\omega^2]$ is the renormalization constant [1]. Satellites in the Ni XPS of NiO have been studied extensively using local CI methods [18,41,42]. Figure 3 shows a fit to experimental Ni $1s$ XPS of NiO (black dashes) compared to our calculations (red) [39]. The quasiparticle peak (at 0 eV) and the largest satellite at ≈ -7 eV are in semiquantitative agreement with experiment, although that peak is weakly split in the theory. The theory also

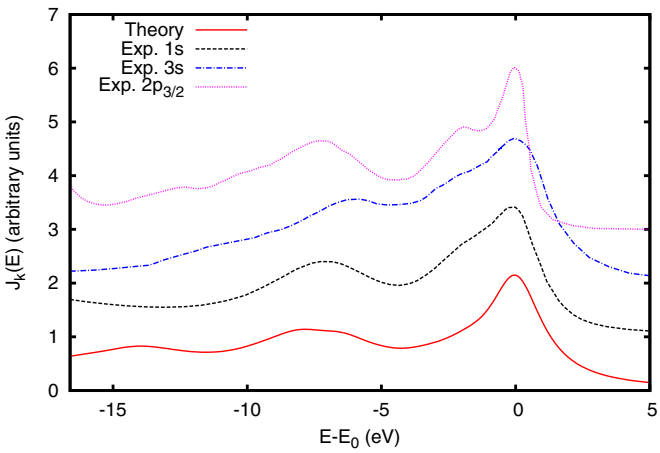

FIG. 3. (Color online) Calculated Ni $1s$ core-level XPS for NiO (bottom) vs a fit to $1s$ (black dashes) [39], $3s$ XPS (blue dotted-dashed), and $2p_{3/2}$ (pink dotted) experimental results [40]. The plots are shifted vertically for clarity.

TABLE I. Relative energy of the first three satellites in the XPS of NiO calculated with RT-TDDFT and NOCI and from experiment. Note that our RT-TDDFT calculation is for the Ni 1*s* XPS, while the NOCI is for Ni 3*s*.

1*s*		3*s*	
RT-TDDFT	Expt.	NOCI	Expt.
1.9	1.5	2.0	2.2
6.5, 7.9	7.2	7.7	6.1
14.0		8.1	10.2

exhibits the secondary peak in the experiment at about −1.5 eV, but the calculated amplitude is much smaller. For reference, the experimental Ni $2p_{3/2}$ and 3*s* XPS are also shown [40]. The higher-energy resolution of the $2p_{3/2}$ spectrum allows a more detailed analysis. For example, the difference in energy and strength of the second major satellite may signify a role of either the core-hole shape or the core-valence exchange interaction [43]. We also compared with calculations for NiO based on the nonorthogonal configuration interaction (NOCI) method [41]. However, this comparison is only qualitative, as our results are for the 1*s* XPS while those with NOCI are for the 3*s*, where exchange with the valence states is more important. Table I (left side) shows the energies of the dominant satellites relative to the main peak from our RT-TDDFT calculation and 1*s* XPS experiment, and (right side) NOCI results for 3*s* excitation energies compared to 3*s* XPS [41]. The agreement between our RT-TDDFT calculations and experiment for the first two major excitations is reasonably good. The third peak is a few eV higher than in the 3*s* experiment and not visible in the 1*s*.

In conclusion, we have developed an efficient approach for calculations of XPS based on a cumulant expansion of the core-hole spectral function with an RT-TDDFT calculation of the cumulant. The approach provides a semiquantitative interpretation of the dominant XPS satellites in terms of local density fluctuations, and yields good results for correlated systems such as NiO and TiO_2. By explicitly treating the dynamic density response of a deep core hole, the approach approximates effects of a nonadiabatic kernel missing in conventional TDDFT treatments of spectra. While the cumulant representation is formally similar to that used for valence XPS, the ingredients and methodology are quite different. Our approach for the core XPS is implemented with an RT-TDDFT calculation of the cumulant in real space, whereas previous treatments of valence XPS were done in reciprocal and frequency space, with a random phase approximation (RPA) calculation of the excitation spectrum and the G_0W_0 approximation for the cumulant. We have also shown that the CT excitations can be interpreted physically by inspection of the dynamic response in real space. This response is characterized by several time scales including an initial transient response followed by oscillatory charge transfer between the core and the ligand orbitals. The method may also be used to extract parameters, e.g., for CT multiplet or tight-binding models [15,16,39,44]. In addition, it may be possible to treat more general quasibosonic excitations, including extrinsic losses and interference [13]. Further analysis of the real-time densities and wave functions could allow quantification of CT and polarization effects as well as other types of neutral excitations. Future plans also include the development of improved core-hole potentials and extensions to treat exchange and multiplet effects.

We thank P. Bagus, G. Bertsch, J. Freericks, A. Lee, and L. Reining for useful comments. This work was supported by DOE Grant No. DE-FG03-97ER45623 (J.J.R. and J.J.K.) and DOE BES DMSE Award No. 10122 (S.A.C.), and was facilitated by the DOE Computational Materials Science Network. One of us (J.J.R.) also thanks the the Kavli Institute for Theoretical Physics at UCSB and the Laboratoire des Solides Irradiés, École Polytechnique, CNRS, Palaiseau, France for hospitality where parts of this work were carried out.

[1] L. Hedin, J. Phys.: Condens. Matter **11**, R489 (1999).
[2] C. N. Berglund and W. E. Spicer, Phys. Rev. **136**, A1030 (1964).
[3] C. Caroli, D. Lederer-Rozenblatt, B. Roulet, and D. Saint-James, Phys. Rev. B **8**, 4552 (1973).
[4] J. J. Chang and D. C. Langreth, Phys. Rev. B **5**, 3512 (1972).
[5] D. Sokcevic, M. Sunjik, and C. Fadley, Surf. Sci. **82**, 383 (1979).
[6] C.-O. Almbladh, Phys. Scr. **32**, 341 (1985).
[7] C.-O. Almbladh, Phys. Rev. B **34**, 3798 (1986).
[8] J. E. Inglesfield, Solid State Commun. **40**, 467 (1981).
[9] J. E. Inglesfield, J. Phys. C **16**, 403 (1983).
[10] L. Hedin, J. Michiels, and J. Inglesfield, Phys. Rev. B **58**, 15565 (1998).
[11] W. Bardyszewski and L. Hedin, Phys. Scr. **32**, 439 (1985).
[12] F. Aryasetiawan, L. Hedin, and K. Karlsson, Phys. Rev. Lett. **77**, 2268 (1996).
[13] M. Guzzo, G. Lani, F. Sottile, P. Romaniello, M. Gatti, J. J. Kas, J. J. Rehr, M. G. Silly, F. Sirotti, and L. Reining, Phys. Rev. Lett. **107**, 166401 (2011).
[14] J. Lischner, D. Vigil-Fowler, and S. G. Louie, Phys. Rev. Lett. **110**, 146801 (2013).
[15] F. de Groot and A. Kotani, *Core Level Spectroscopy of Solids* (CRC Press, Boca Raton, FL, 2008).
[16] J. D. Lee, O. Gunnarsson, and L. Hedin, Phys. Rev. B **60**, 8034 (1999).
[17] H. Ikeno, T. Mizoguchi, and I. Tanaka, Phys. Rev. B **83**, 155107 (2011).
[18] P. S. Bagus, G. Pacchioni, and F. Parmigiani, Chem. Phys. Lett. **207**, 569 (1993).
[19] P. Bagus, C. Nelin, E. Ilton, M. Baron, H. Abbott, E. Primorac, H. Kuhlenbeck, S. Shaikhutdinov, and H.-J. Freund, Chem. Phys. Lett. **487**, 237 (2010).
[20] M. W. Haverkort, M. Zwierzycki, and O. K. Andersen, Phys. Rev. B **85**, 165113 (2012).
[21] M. Guzzo, J. Kas, F. Sottile, M. Silly, and F. Sirotti, Eur. Phys. J. B **85**, 1 (2012).
[22] L. Hedin, Phys. Rev. **139**, A796 (1965).

[23] P. Nozières and C. T. de Dominicis, Phys. Rev. **178**, 1097 (1969).
[24] D. C. Langreth, Phys. Rev. B **1**, 471 (1970).
[25] K. Yabana and G. F. Bertsch, Phys. Rev. B **54**, 4484 (1996).
[26] K. Yabana, T. Nakatsukasa, J.-I. Iwata, and G. F. Bertsch, Phys. Status Solidi B **243**, 1121 (2006).
[27] Y. Takimoto, F. D. Vila, and J. J. Rehr, J. Chem. Phys. **127**, 154114 (2007); See also A. Tsolakidis, D. Sánchez-Portal, and R. M. Martin, Phys. Rev. B **66**, 235416 (2002).
[28] F. D. Vila, D. A. Strubbe, Y. Takimoto, X. Andrade, A. Rubio, S. G. Louie, and J. J. Rehr, J. Chem. Phys. **133**, 034111 (2010).
[29] T. Otobe, K. Yabana, and J.-I. Iwata, J. Comput. Theor. Nanosci. **6**, 2545 (2009).
[30] A. J. Lee, F. D. Vila, and J. J. Rehr, Phys. Rev. B **86**, 115107 (2012).
[31] G. van der Laan, C. Westra, C. Haas, and G. A. Sawatzky, Phys. Rev. B **23**, 4369 (1981).
[32] J. Crank and P. Nicolson, Math. Proc. Cambridge **43**, 50 (1947).
[33] J. M. Soler, E. Artacho, J. D. Gale, A. García, J. Junquera, P. Ordejón, and D. Sánchez-Portal, J. Phys.: Condens. Matter **14**, 2745 (2002).
[34] N. Vast, L. Reining, V. Olevano, P. Schattschneider, and B. Jouffrey, Phys. Rev. Lett. **88**, 037601 (2002).
[35] K. Okada and A. Kotani, J. Electron Spectrosc. Relat. Phenom. **62**, 131 (1993).
[36] D. K. G. de Boer, C. Haas, and G. A. Sawatzky, Phys. Rev. B **29**, 4401 (1984).
[37] M. Niwano, S. Sato, T. Koide, T. Shidara, A. Fujimori, H. Fukutani, S. Shin, and M. Ishigame, J. Phys. Soc. Jpn. **57**, 1489 (1988).
[38] A. Bianconi, T. Miyahara, A. Kotani, Y. Kitajima, T. Yokoyama, H. Kuroda, M. Funabashi, H. Arai, and T. Ohta, Phys. Rev. B **39**, 3380 (1989).
[39] M. Calandra, J. P. Rueff, C. Gougoussis, D. Céolin, M. Gorgoi, S. Benedetti, P. Torelli, A. Shukla, D. Chandesris, and C. Brouder, Phys. Rev. B **86**, 165102 (2012).
[40] S. Altieri, L. H. Tjeng, A. Tanaka, and G. A. Sawatzky, Phys. Rev. B **61**, 13403 (2000).
[41] L. Hozoi, A. de Vries, R. Broer, C. de Graaf, and P. Bagus, Chem. Phys. **331**, 178 (2006).
[42] P. S. Bagus, R. Broer, and E. S. Ilton, J. Electron Spectrosc. Relat. Phenom. **165**, 46 (2008).
[43] P. S. Bagus and E. S. Ilton, Phys. Rev. B **73**, 155110 (2006).
[44] E. Klevak, J. J. Kas, and J. J. Rehr, Phys. Rev. B **89**, 085123 (2014).